Wavelets meet Burgulence: CVS-filtered Burgers equation

Romain Nguyen van yen [a,*], Marie Farge [a], Dmitry Kolomenskiy [b], Kai Schneider [b], Nick Kingsbury [c]

[a] *LMD–CNRS, École Normale Supérieure, Paris, France*
[b] *M2P2–CNRS & CMI, Université de Provence, Marseille, France*
[c] *Signal Processing Group, Department of Engineering, Cambridge University, UK*

Abstract

Numerical experiments with the one-dimensional inviscid Burgers equation show that filtering the solution at each time step in a way similar to CVS (Coherent Vortex Simulation) gives the solution of the viscous Burgers equation. The CVS filter used here is based on a complex-valued translation-invariant wavelet representation of the velocity, from which one selects the wavelet coefficients having modulus larger than a threshold whose value is iteratively estimated. The flow evolution is computed from either deterministic or random initial conditions, considering both white noise and Brownian motion.
© 2008 Elsevier B.V. All rights reserved.

PACS: 47.27.Eq

Keywords: Burgers equation; Wavelets; Coherent vortex simulation

1. Introduction

The fully-developed turbulent regime is described by solutions of the Navier–Stokes equations for two or three-dimensional incompressible fluids, in the limit where the kinematic viscosity becomes very small. By analogy, Burgulence is described by the solutions of Burgers equations for a one–dimensional fluid in the same limit, as first proposed by Burgers [3] and advocated by von Neumann [19]. This toy model for turbulence has been extensively used since then [1, 13,15,21,23]; Frisch and Bec have proposed to name it: *Burgulence* [11].

We consider the one-dimensional Burgers equation in a periodic domain of support $x \in [-1, 1]$, which describes the space–time evolution of the velocity $u(x, t)$ of a one-dimensional fluid flow:

$$\partial_t u + \frac{1}{2}\partial_x u^2 = \nu\partial_{xx}u, \tag{1}$$

supplemented with a suitable initial condition and where ν denotes the kinematic viscosity. The solutions of (1) can be computed analytically using the Cole–Hopf transformation [4, 6,14]. When $\nu \to 0$ the solutions of the viscous Burgers equation approach weak solutions of the inviscid problem. The uniqueness of these solutions stems from the condition that shocks have negative jumps, which guarantees energy dissipation. For Burgers equation, this condition is equivalent to an entropy condition [12,17,18,20].

The wavelet representation has been proposed for studying turbulence [7], since it preserves both the spatial and spectral structure of the flow by realizing an optimal compromise in regard of the uncertainty principle. We have found that projecting the vorticity field onto a wavelet basis, and retaining only the strongest coefficients, extracts the coherent structures out of fully-developed turbulent flows [8,9]. We have then proposed a computational method for solving the Navier–Stokes equations in wavelet space [8]. We have shown that extracting the coherent contribution at each time step preserves the nonlinear dynamics, whatever its scale of activity, while discarding the incoherent contribution corresponds to turbulent dissipation [22]. This is the principle of the CVS (Coherent Vortex Simulation) method we have proposed [8,10].

The aim of the present paper is to apply the CVS filter to the inviscid Burgers equation and check if this is equivalent

---

* Corresponding author.
E-mail addresses: rnguyen@lmd.ens.fr (R. Nguyen van yen),
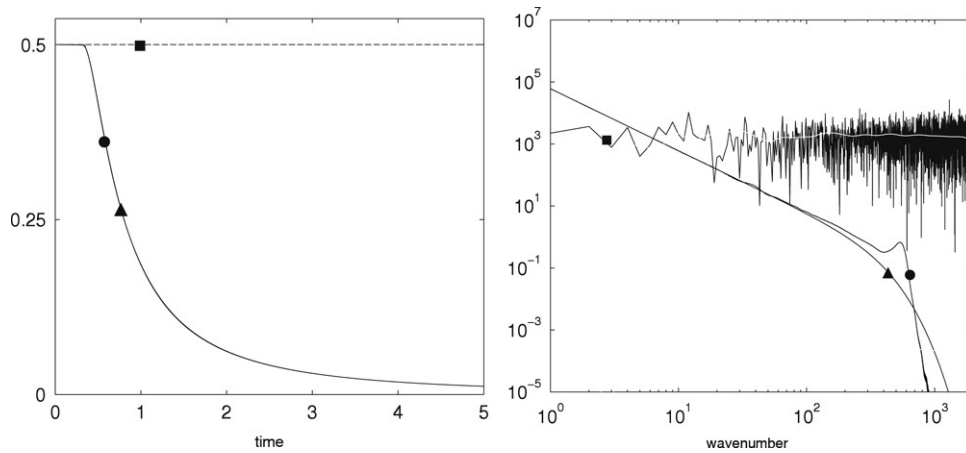farge@lmd.ens.fr (M. Farge).

Fig. 1. Deterministic initial conditions. Left: Time evolution of energy. Right: Energy spectrum at $t = 5$. We compare the Galerkin-truncated inviscid (square), viscous (triangle) and CVS-filtered inviscid (circle) cases. We observe that for the inviscid case (right) the wavelet spectrum (white line) better exhibits the energy equipartition than the Fourier spectrum (black line).

to solving the viscous Burgers equation. The outline is the following. First we recall the principle of CVS filtering and its extension using complex-valued translation-invariant wavelets. The numerical scheme is described briefly and the main part presents results of several numerical experiments, considering either deterministic or random initial conditions. Finally, we draw conclusions and propose some perspectives.

2. Numerical method

The Burgers equation (1) is discretized on N grid points using a Fourier spectral collocation methods,

$$\frac{\partial U}{\partial t} + \frac{1}{3}D_N(U^2) + \frac{1}{3}U \cdot D_N(U) - \nu D_N^2(U) = 0, \qquad (2)$$

where U approximates $(u(x_0, t), u(x_1, t), \ldots, u(x_{N-1}, t))$, D_N stands for the Fourier collocation differentiation and $\cdot$ is the pointwise product of two vectors. The discretization of the nonlinear term in (2) is chosen in order to conserve the kinetic energy $E = \frac{1}{2}\int_{-1}^{1} u^2(x, t)dx$ when $\nu = 0$ [5]. For time integration a fourth-order Runge–Kutta scheme is used.

At each time step we filter the solution using the CVS method, which we now recall briefly. Given orthogonal wavelets (ψ_{ji}) and the associated scaling function at the largest scale φ, the velocity can be expanded into

$$u(x) = \langle u \mid \varphi \rangle \varphi(x) + \sum_{j=0}^{J-1}\sum_{i=1}^{2^j} \langle u \mid \psi_{ji} \rangle \psi_{ji}(x), \qquad (3)$$

where j is the scale index, i is the position index and the inner product is $\langle a \mid b \rangle = \int_{-1}^{1} a(x) \cdot b^*(x)dx$ with b^* denoting the complex conjugate of b. Since location in orthogonal wavelet space is sampled on a dyadic grid, this representation breaks the local translation invariance of (1) which may impair the stability of the numerical scheme. Therefore we prefer using, instead of real-valued wavelets, complex valued wavelets [16] which very closely preserve translation invariance. In this case, (3) still holds as long as we replace the right-hand side by its real part.

The CVS filter then consists in discarding the wavelet coefficients whose modulus is below a threshold T. In addition, wavelet coefficients at the finest scale are systematically filtered out to avoid aliasing errors. The resulting velocity u_T is a nonlinear approximation of u.

Because the velocity field decays in time, the threshold has to be estimated at each time step in a self-consistent way. To do this, we follow the iterative method introduced in [2], which consists in imposing the ratio between the standard deviation of the discarded wavelet coefficients and the threshold itself,

$$T^2 = \frac{5}{N_T}\sum_{j=0}^{J-1}\sum_{i=1}^{2^j} |\widetilde{u}_{ji}|^2 \, H(T - |\widetilde{u}_{ji}|), \qquad (4)$$

where H is the Heaviside step function and N_T is the number of wavelet coefficients below the threshold. The solution of (4) is determined numerically using a fixed point iterative procedure [2], initialized with $T_0 = 5E/N$, where E is the total energy.

3. Deterministic initial condition

We consider Burgers equation (1) with the deterministic initial condition $u(t = 0, x) = -\sin(\pi x)$. We begin by comparing three computations: a Galerkin-truncated inviscid case ($\nu = 0$), a viscous case ($\nu = 10^{-4}$), and an inviscid case with the CVS filter applied at each time step. The solutions are computed up to time $t = 5$, using $N = 4096$ grid points.

By computing in the Galerkin-truncated inviscid case ($\nu = 0$), we check that our numerical scheme conserves energy (Fig. 1, left) as theoretically predicted. We observe that the final solution at $t = 5$ exhibits energy equipartition (Fig. 1, right) with a Gaussian velocity PDF, as expected. Note that the white line in Fig. 1 (right) corresponds to the wavelet energy spectrum, *i.e.*, the squared modulus of the wavelet coefficients computed with a complex-valued Morlet wavelet. It better exhibits the k^0 scaling, characteristic of the energy equipartition, than the highly oscillatory Fourier energy spectrum (black line). This illustrates the fact that the wavelet energy spectrum is more stable than the Fourier energy
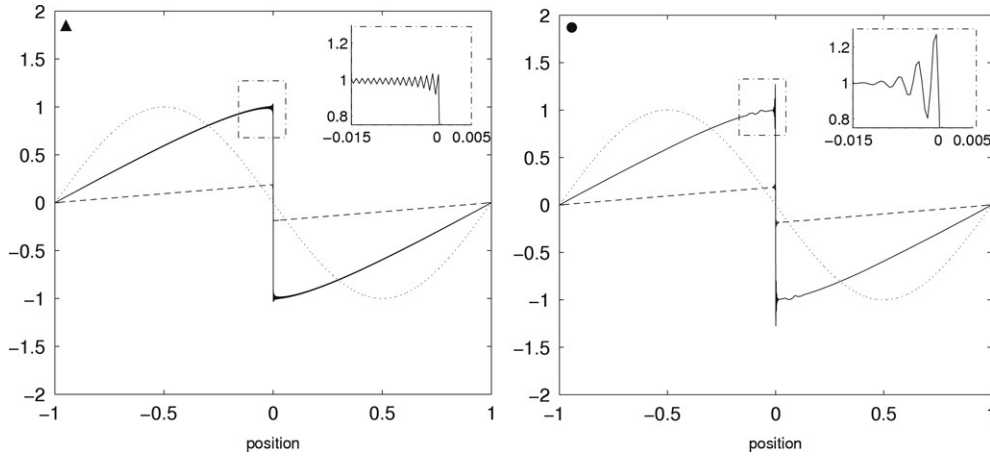
Fig. 2. Deterministic initial conditions. Snapshots of velocity for the viscous (left) and the CVS-Filtered inviscid (right) cases at $t = 0$ (dotted line), $t = 0.5$ (solid line) and $t = 5$ (dashed line). The insets show a zoom of the shock at $t = 0.5$.
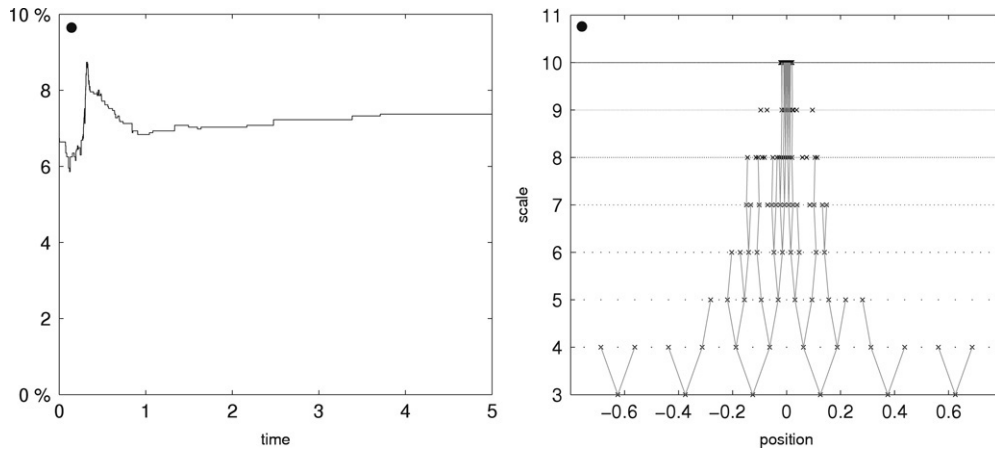

Fig. 3. Deterministic initial conditions. Left: Time evolution of the percentage of wavelet coefficients retained after filtering. Right: Dyadic tree of the wavelet coefficients which are retained after filtering at $t = 5$. The crosses indicate the $7\%N$ retained wavelet coefficients, while the small dots correspond to the $93\%N$ discarded wavelet coefficients. The scale varies from coarse to fine, up the vertical axis.

spectrum when we analyse only one realization of a stochastic process [7].

For the viscous and CVS-filtered inviscid cases, the energy remains basically constant until the shock forms at $t = 1/\pi$, but then decays with a t^{-2} law. In Fig. 1 (right) the energy spectra of the viscous and CVS-filtered inviscid cases exhibit a power law behaviour with slope -2.

Fig. 2 shows the velocity at three time instants for the viscous and CVS-filtered inviscid cases. The CVS-filtered inviscid solution follows the same dynamics as the viscous one, except for the small overshoot we observe at $x = 0$ after the shock has formed. This Gibbs phenomenon is stronger but less oscillatory for the CVS-filtered inviscid case than for the viscous case (see the insets in Fig. 2).

The time evolution of the percentage of retained wavelet coefficients is presented in Fig. 3 (left). It shows that, with only relatively few coefficients (about $7\%N$), we are able to track the nonlinear dynamics of the flow and this number remains almost constant after the shock formation. At $t = 5$, the retained wavelet coefficients are located around $x = 0$, the position

of the shock, and span all scales there, as illustrated in Fig. 3 (right).

We now show that, when N increases, the filtered solutions converge towards the entropy solution u_{ref} which solves the Burgers equation in the inviscid limit. For comparison, we also consider viscous solutions with viscosity depending on N ($\nu = 0.4096N^{-1}$), which are known to converge to u_{ref} everywhere, except at $x = 0$. The entropy solution u_{ref} is directly calculated using the method of characteristics.

First, we consider a global error estimate, the relative mean square error, defined as

$$\epsilon_N(t) = \frac{\|u - u_{\text{ref}}\|_2^2}{\|u_{\text{ref}}\|_2^2}. \tag{5}$$

On Fig. 4(left) we plot $\epsilon_N(t)$ for $N = 4096$. The error for the CVS-filtered inviscid case is larger but saturates after $t \simeq 2$. In contrast, the error for the viscous case keeps increasing because the finite viscosity smooths the shock away. Considering now $t = 5$ and varying N, we find that for both the viscous
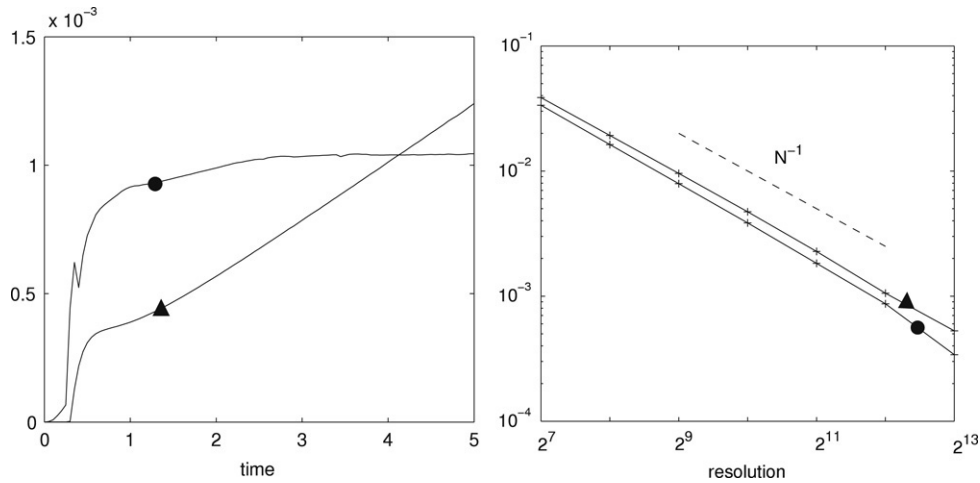
Fig. 4. Deterministic initial conditions. Left: Time evolution of the relative mean squared error ϵ_N at $N = 4096$. Right: Relative mean squared error ϵ_N at $t = 5$ for different numerical resolutions, $N = 128$ to $N = 8192$. We compare the viscous (triangle) and CVS-filtered inviscid (circle) cases.
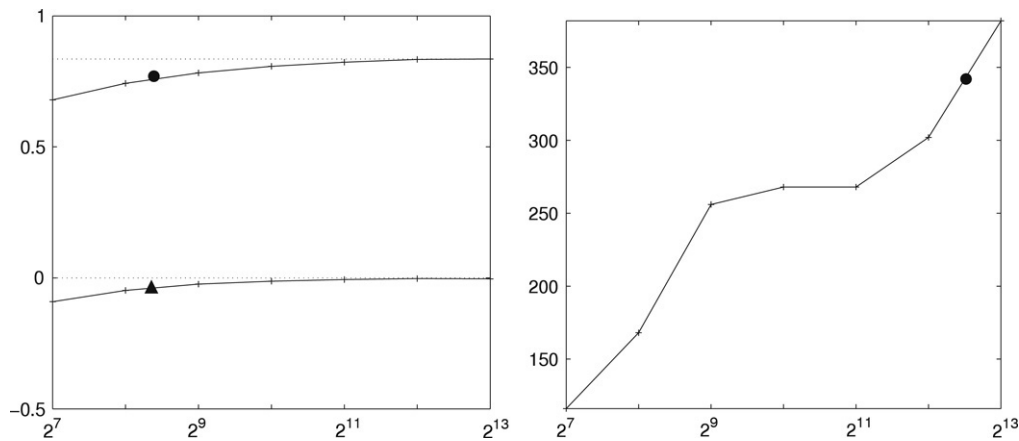

Fig. 5. Deterministic initial conditions. Error on the relative total variation ϵ'_N (left), and number of retained wavelet coefficients (right), as functions of N at $t = 5$, for the viscous (triangle) and CVS-filtered inviscid (circle) solutions.

and CVS-filtered inviscid cases ϵ_N decreases as N^{-1} (Fig. 4, right).

We now study the behaviour of the oscillations in the neighbourhood of the shock when the resolution N is increased. The total variation of a function f on $[-1, 1]$ is defined by:

$$\|f\|_{TV} = \int_{-1}^{1} |\partial_x f| \mathrm{d}x. \tag{6}$$

To detect the presence of spurious oscillations, we compute the relative error on the total variation.

$$\epsilon'_N(t) = \frac{\|u(x, t)\|_{TV} - \|u_{\text{ref}}(x, t)\|_{TV}}{\|u_{\text{ref}}(x, t)\|_{TV}}, \tag{7}$$

which is plotted as a function of N for $t = 5$ on Fig. 5 (left). For the viscous case, ϵ'_N is negative and converges towards zero when N increases. For the CVS-filtered inviscid case, ϵ'_N tends to a finite positive value close to 0.84. The overshoot that could be seen on Fig. 2 persists but becomes more and more localized around the singularity when N increases, thus ensuring mean square convergence.

Let us end this section by a short discussion on the evolution of the compression rate when N increases. Fig. 5 (right)

shows that the number of retained wavelet coefficients increases roughly logarithmically as a function of N. As a consequence, notice that for the filtered solution the relative mean square error $\epsilon_N(t)$, if it is considered as a function of the number of retained coefficients only, converges to zero exponentially fast. However, to experience this promising rate of convergence in practice, we should compute the evolution of u using only the wavelet coefficients whose modulus remains above the threshold.

4. Random initial condition

In the previous section we demonstrated that the CVS-filtered inviscid Burgers equation exhibits an evolution similar to that of the viscous Burgers equation. We now would like to check if this is still verified in the context of *Burgulence* for both white noise [1] and Brownian motion [21].

4.1. White-noise initial condition

We take as initial velocity one realization of a Gaussian white noise computed at resolution $N = 4096$, which corresponds to a random non-intermittent initial condition.
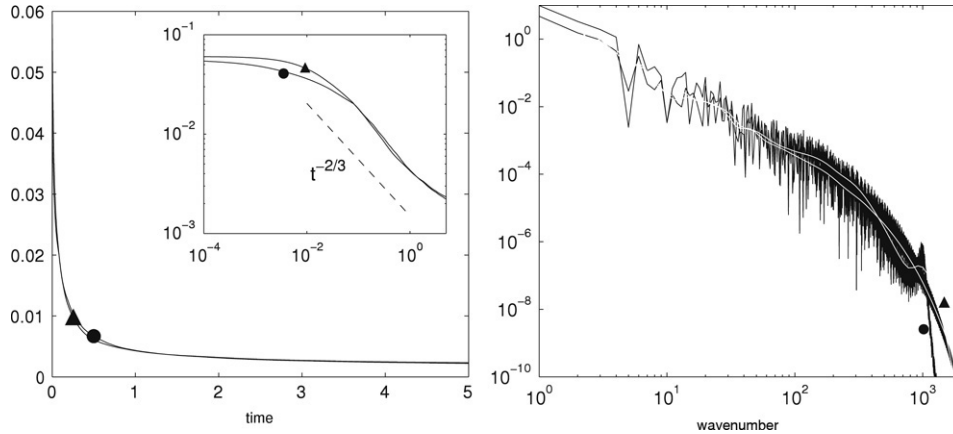
Fig. 6. White noise initial conditions. Left: Time evolution of energy. The inset shows the $t^{-2/3}$ decay in log–log coordinates. Right: energy spectrum at $t = 5$. We compare the viscous (triangle) and CVS-filtered inviscid (circle) simulations. We observe that the wavelet spectrum (white lines) better exhibits the k^{-2} scaling of energy than the Fourier spectrum (black lines).
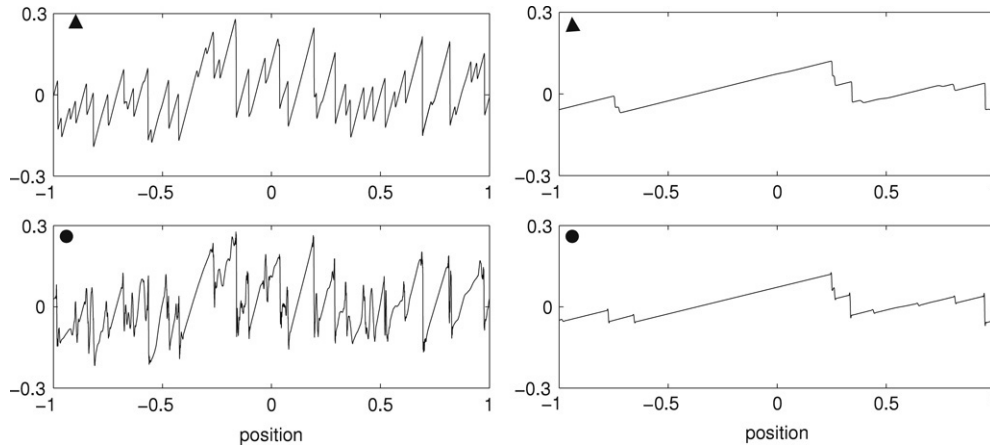

Fig. 7. White noise initial conditions. Snapshots of velocity at $t = 0.3$ (left) and $t = 5$ (right). Top: viscous equation with $\nu = 2 \times 10^{-5}$. Bottom: CVS-filtered inviscid equation.

Since the CVS filter removes the non-intermittent noisy contributions, if applied to a Gaussian white noise the latter would be completely filtered out. Therefore we first integrate the viscous equation with $\nu = 2 \times 10^{-5}$ without filtering, and wait until the flow intermittency has sufficiently developed before applying the filter. To check the flow intermittency we monitor the flatness of the velocity gradient until it reaches the value 20, which happens at $t = 0.017$ for the realization described here. Then, we reset $t = 0$ and integrate up to $t = 5$, both the viscous equation with $\nu = 2 \times 10^{-5}$, and the CVS-filtered inviscid equation.

In Fig. 6 (left) we show that the energy, for both the CVS-filtered inviscid solution and the viscous solution, decays with a $t^{-2/3}$ law, as found by Burgers [4,21]. In Fig. 6 (right) we observe at $t = 5$ that both energy spectra present the same k^{-2} scaling. Notice that the two white lines in Fig. 6 (right) correspond to the wavelet energy spectrum, which better exhibits the k^{-2} scaling of the energy than the highly oscillatory Fourier energy spectrum (black lines).

Finally, we show on Fig. 7 that the viscous and CVS-filtered inviscid solutions are almost identical in physical

space, presenting a typical sawtooth profile as first noticed by Burgers [4].

4.2. Brownian motion initial condition

We use the same resolution $N = 4096$ as above, but only the initial condition changes. Since we have chosen periodic boundary conditions we approximate the Brownian motion by the Fourier series:

$$u(x, 0) = \mathrm{Re}\left(\sum_k \widehat{u_k} e^{ikx} \right) \tag{8}$$

where $k = -\frac{N}{2} + 1, -\frac{N}{2}, \ldots, \frac{N}{2} - 1$. We set $\widehat{u_0} = 0$ and, for $k \neq 0$, we take for $\widehat{u_k}$ a complex Gaussian random variable with standard deviation $1/|k|$.

The solution for the viscous case is computed with $\nu = 1.2 \times 10^{-4}$. For the CVS-filtered inviscid case, as we did for the white noise initial condition, we do not filter before enough intermittency has developed. We thus integrate the viscous equation with $\nu = 1.2 \times 10^{-4}$ for 0.05 time units and then switch viscosity off. This procedure provides the initial velocity which, by construction, is the same for both methods (Fig. 8).
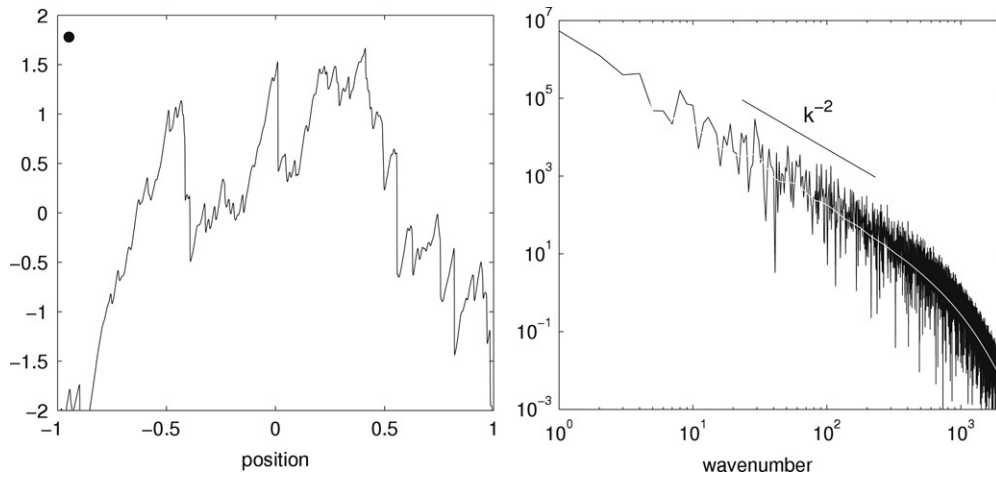
Fig. 8. Brownian initial condition. Velocity at $t = 0$ (left), its Fourier energy spectrum (right, black line) and its wavelet energy spectrum (right, white line).
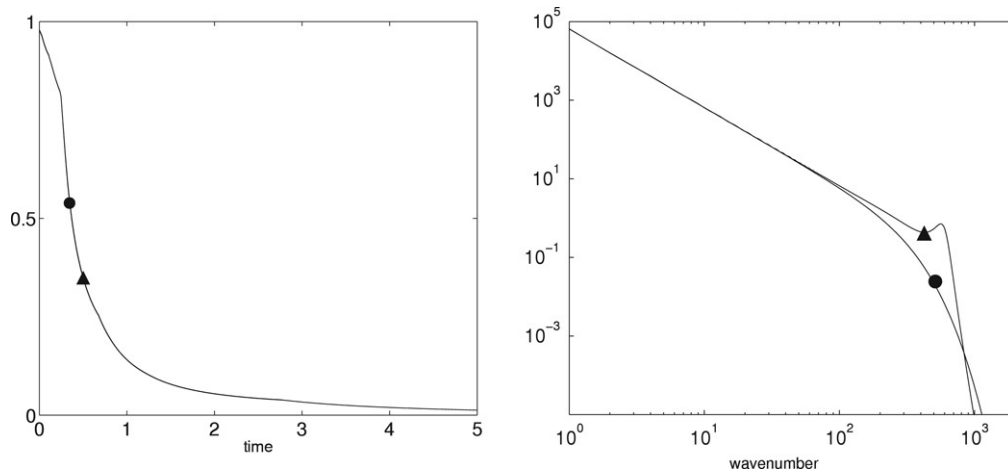

Fig. 9. Brownian initial condition. Left: Time evolution of energy. Right: wavelet energy spectrum at $t = 5$. We compare the viscous (triangle) and CVS-filtered inviscid (circle) cases.
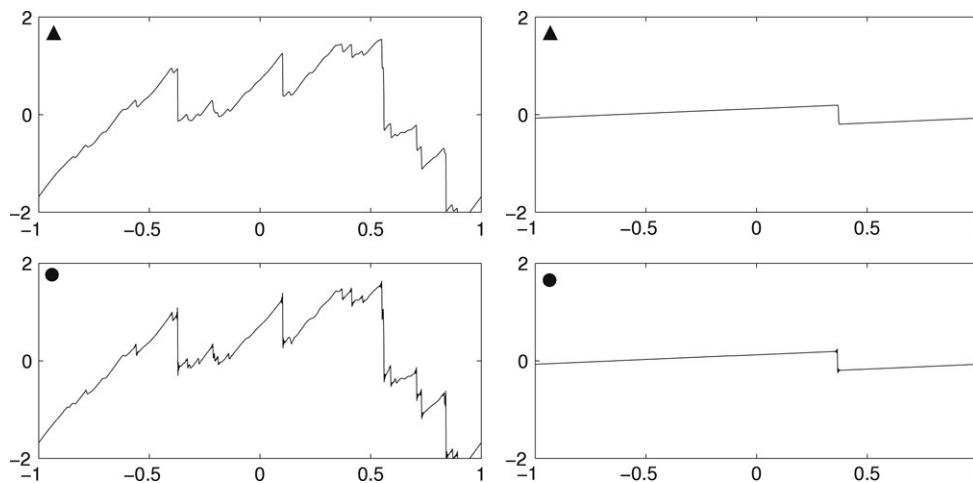

Fig. 10. Brownian initial conditions. Snapshots of velocity at $t = 0.1$ (left) and $t = 5$ (right). Top: viscous equation with $\nu = 1.2 \times 10^{-4}$. Bottom: CVS-filtered inviscid equation.

The energy decay matches well between the CVS-filtered inviscid and the viscous solutions (Fig. 9, left). A k^{-2} power spectrum is also obtained for both at $t = 5$ (Fig. 9, right).

At $t = 0.1$ numerous small shocks are present in the viscous solution (Fig. 10, top left). All of them are correctly reproduced by the CVS-filtered inviscid solution (Fig. 10, bottom left).

At $t = 5$ the single remaining shock, which is still resolved in the viscous solution (Fig. 10, top right), is correctly reproduced in the CVS-filtered inviscid solution (Fig. 10, bottom right).

5. Conclusion

We have shown that CVS filtering at each time step the solution of the inviscid Burgers equation gives the same evolution as the viscous Burgers equation, for both deterministic and random initial conditions. As our contribution to Euler equations' 250th anniversary and Euler's 300th birthday, we conjecture that CVS filtering the Euler equation may be equivalent to solving the Navier–Stokes equations in the fully-developed turbulent regime, *i.e.*, when dissipation has become independent of viscosity. We predict that the retained wavelet coefficients would preserve Euler's nonlinear dynamics, while discarding the weaker wavelet coefficients would model turbulent dissipation and give Navier–Stokes solutions. Since in the fully-developed turbulent regime turbulent dissipation strongly dominates molecular dissipation, there is no reason to model turbulent dissipation by a Laplace operator anymore. Indeed, turbulent dissipation is a property of the flow, while molecular dissipation is a property of the fluid and may no more play a role when turbulence is fully-developed. We think that in this regime the CVS filter could be a better way to model dissipation, replacing global by local smoothing, while preserving nonlinear interactions. In this paper we have chosen the simplest toy model to test this conjecture, although Burgers' equation, in contrast to Euler's equation, is neither chaotic nor produces randomness. Therefore we conjecture that the CVS-filter would work better for Euler/Navier–Stokes than for Burgers, since CVS is based on denoising which is justified when there is chaos and randomness.

Acknowledgments

References

[1] M. Avellaneda, W.E. , Commun. Math. Phys. 172 (1995) 13–38.
[2] A. Azzalini, M. Farge, K. Schneider, Appl. Comput. Harmon. Anal. 18 (2) (2005) 177–185.
[3] J.M. Burgers, Verh. KNAW, Afd. Natuurkunde, XVII 2 (1939) 1–53.
[4] J.M. Burgers, Proc. KNAW B, LVII 1 (1954) 45–72.
[5] C. Canuto, M.Y. Hussaini, A. Quarteroni, T.A. Zang, Spectral Methods in Fluid Dynamics, Springer-Verlag, 1988.
[6] J.D. Cole, Q. Appl. Math. 9 (1951) 225.
[7] M. Farge, Ann. Rev. Fluid Mech. 24 (1992) 395–457.
[8] M. Farge, K. Schneider, N. Kevlahan, Phys. Fluids 11 (8) (1999) 2187–2201.
[9] M. Farge, G. Pellegrino, K. Schneider, Phys. Rev. Lett. 87 (5) (2001) 45011–45014.
[10] M. Farge, K. Schneider, Flow, Turb. Combus. 66 (4) (2001) 393–426.
[11] U. Frisch, J. Bec, New trends in turbulence, in: M. Lesieur, A. Yaglom, F. David (Eds.), in: Les Houches 2000, vol. 74, Springer, 2002, p. 341.
[12] P. Germain, R. Bader, Note technique ONERA, OA no 1/1711-1, May 1953.
[13] S.N. Gurbatov, S.I. Simdyankin, E. Aurell, U. Frisch, G. Tóth, J. Fluid Mech. 344 (1997) 339–374.
[14] E. Hopf, Comm. Pure Appl. Math. 3 (1950) 201.
[15] S. Kida, J. Fluid Mech. 79 (1997) 337–377.
[16] N. Kingsbury, Appl. Comput. Harmon. Anal. 10 (3) (2001) 234–253.
[17] S.N. Kruzhkov, Math. USSR Sb. 10 (2) (1970) 217–243; Amer. Math. Transl. Ser. 2 26, 95–172.
[18] P.-D. Lax, Comm. Pure Appl. Math. 7 (1954) 159–193.
[19] J. von Neumann, in: A.H. Taub (Ed.), Collected Works, vol. 5, Pergamon, 1961, pp. 437–471.
[20] O. Oleinik, Usp. Mat. Nauk 12 (3) (1957) 3–73; Amer. Math. Transl. Ser. 2 26, 95–172.
[21] Z.S. She, E. Aurell, U. Frisch, Commun. Math. Phys. 148 (1992) 623–641.
[22] K. Schneider, M. Farge, G. Pellegrino, M. Rogers, J. Fluid Mech. 534 (2005) 39–66.
[23] M. Vergassola, B. Dubrulle, U. Frisch, A. Noullez, Astron. Astrophys. 289 (1994) 325–356.